Fourteenth USA/Europe Air Traffic Management Research and Development Seminar (ATM2021)

Safety risk posed to persons on the ground by commercial UAS-based services

Learning from airports and hazardous installations

Henk A.P. Blom
Aerospace Engineering Dept.
Delft University of Technology
Delft, Netherlands
h.a.p.blom@tudelft.nl

Chengpeng Jiang
Aerospace Engineering Dept.
Delft University of Technology
Delft, Netherlands
c.jiang@tudelft.nl

***Abstract*—The unique capabilities of an Unmanned Aircraft System (UAS) creates opportunities for commercial services. The key question is what is an acceptable level of risk posed to third parties on the ground that have no direct benefit from commercial UAS flights. In literature the common view is that an acceptable level of Third Party Risk (TPR) posed by UAS operations follows from an Equivalent Level Of Safety (ELOS) criterion, which means that per flight hour a UAS should not pose more safety risk to persons on the ground than a commercial aircraft does. However in commercial aviation there are also TPR indicators in use that are directed to accident risk posed by all annual commercial flights to the population around an airport. These population directed indicators find their origin in TPR posed by hazardous installations to its environment. The aim of this paper is to improve the understanding of risk posed to the population by annual UAS-based services through learning from TPR knowledge and regulation for airports and hazardous installations. As main result this paper develops an analytical approach to evaluate the annual risk posed by a commercial UAS-based parcel delivery service in urban and metropolitan areas. The obtained results show that the TPR indicators that stem from hazardous installations and airports provide novel insight regarding TPR of commercial UAS-based service.**

Keywords- Collective risk; Fatality risk; Individual risk; Parcel delivery; Third party risk; Unmanned aircraft

I. INTRODUCTION

An Unmanned Aircraft System (UAS) [1] has technically the ability to replace manned aircraft and aerial platforms. This capability is of particular interest for commercial UAS-based taxi services, parcel delivery services, medical aid services, etc. As has been identified in a recent EASA conducted study [2], the advantages of commercial UAS-based services may come with negative issues for overflown population. The negative issues identified are safety risks, noise hindrance, visual pollution and other environmental impact, as well as privacy, security and cyber-security concerns. The development of these commercial UAS-based services encounters a yet unresolved gap: many potential customers live in urban and metropolitan areas where these issues play a key role. In line with this, standing safety regulations typically consider UAS not (yet) safe enough to be allowed to fly to these potential customers [3-5]. To abridge the safety gap there is need for the development and design of more reliable UAS, e.g. [6], other support systems that enable safe UAS operations, e.g. [7-10], as well as an Urban Air Mobility (UAM) framework, e.g. [2, 11] that allows flying Beyond Visual Line of Sight (BVLOS). A contributing role in closing this gap is developing a better understanding of UAS posed safety risks, e.g. [12, 13].

Safety risk posed by a UAS flight to persons on the ground has been well studied [14-17]. The common finding is that the risk posed per UAS flight hour to persons on the ground should be at an Equivalent Level Of Safety (ELOS) than the TPR posed per flight hour by a commercial aircraft. Commercial aviation accident data has been used to assess the ELOS criterion at 0.76×10^{-7} fatalities on the ground per flight hour [17]. Because the ELOS criterion is fixed per flight hour, it means that the overall UAS system failure rate λ_E has to increase linearly with the density of the population that is overflown. In addition to population density and λ_E, other factors also play a role in TPR analysis, such as UAS type, size of crash area, probability of fatality for an unprotected person in the crash area and shelter protection factor. Melnyk et al. [18] provides an overview of this accumulated knowledge, and subsequently uses this for the assessment of prospectively calculated TPR per flight hour for flying various types of UAS over various population densities. For UAS operations in an urban area the derived requirements on overall UAS system failure rate range from 3.42×10^{-4} per flight hour for a mini UA ($\leq$ 2 kg), to 2.01×10^{-8} per flight hour for a heavy UA (> 4550 kg). For a metropolitan city center these ELOS derived requirements are an order of magnitude more stringent. More recently it has been shown that with increasing UAS traffic a significant contribution to λ_E may stem from UAS crash due to mid-air collision with another UAS [19] or with low-flying general aviation (GA) [20].

In commercial aviation almost all fatalities concern crew and passengers onboard aircraft. This explains why in commercial aviation the ELOS reference of expected number

of ground fatalities per flight hour is not a widely used TPR indicator. Instead, TPR indicators are defined from a population perspective in terms of individual risk and societal risk [21, 22]. For these population directed TPR indicators, models have been developed that allow to assess changes in risk posed to persons on the ground due to changes in the amount of flights, new departure/arrival routes, the impact of a new airport, the risk of constructing a residential building in a certain area, etc. Because the same TPR indicators are in use for hazardous facilities [22-27], there is ample experience in setting acceptable thresholds on Individual and Societal risk indicators. This motivated [28] to extend the Individual Risk and Societal risk indicators from conventional aviation to similar versions for UAS operations. In addition, existing TPR simulation models of UAS operations [29-31] have been extended for these novel TPR indicators, and the working of this extended framework has been demonstrated by [28] through simulating a hypothetical UAS-based parcel delivery service in the city of Delft. The simulation results obtained for this hypothetical example show that modelling and assessment of Individual and Societal risk provides significant novel insight over the ELOS adopted TPR indicator. The objective of the current paper is to extend the simulation directed approach of [28] with an analytical approach by adopting the homogeneity assumptions of Melnyk et al. [18]. This analytical approach yields population directed requirements to the overall UAS system failure rate λ_E. These novel λ_E requirements are subsequently shown to differ significantly from the ELOS-based requirements [18].

This paper is organized as follows. Section II reviews existing TPR models for commercial aviation and for UAS operations. Section III reviews the population directed TPR model extension by [28] for UAS operations involving a large number of flights per annum. Section IV develops an analytical approach to obtain λ_E requirements from the population directed TPR models in section III for a UAS-based parcel delivery service, and compares them to the ELOS-based approach. Section V applies the analytical approach of section IV to last-mile delivery in three types of populated areas: urban area, metropolitan area and metropolitan city center. Section VI draws conclusions. A list of symbols is given in Appendix A.

II. TPR IN AVIATION RESEARCH LITERATURE

A. TPR models for commercial aviation

For commercial aviation around airports TPR models have been developed for Individual risk and for Societal risk [21, 22]. These airport directed developments find their basis in TPR research for hazardous facilities [23-27].

Individual risk $R_I(y)$ of commercial air transport is defined as: *"The probability that an average unprotected person, who resides permanently at ground location y, would get killed due to the direct consequences of an aircraft accident during a given annum."*

Characterization of $R_I(y)$ around an airport satisfies [22]:

$$R_I(y) = \sum_d [N_d P(C \mid d)\, p_s(y \mid d) \left|A(d)\right| P(F \mid y \in A(d))] \quad (2.1)$$

with N_d the annual number of flights of type d, $P(C \mid d)$ the accident probability model, $p_s(. \mid d)$ the crash location model, $\left|A(d)\right|$ impact area size, and $P(F \mid y \in A(d))$ the fatality model.

The Individual risk indicator is population-independent, i.e. it does not make any difference if a ground location y is in a rural area or in the center of a city. Individual risk defines risk contours on a location map that can be used for zonal policies regarding any current or future use of a given area that is exposed to non-negligible Individual risk levels.

Safety regulation of hazardous installations and airports in various countries typically adopts an maximum C_{IR} on the acceptable level of $R_I(y)$, e.g. [26, 27]:

$$R_I(y) \le C_{IR} \qquad \text{for all} \qquad y \in Y / Y_{Zone}$$

with Y_{Zone} the zone for which land-use restrictions apply. For example in Y_{Zone} no new housing development is allowed, though waivers may apply for other land-use activities.

To capture societal risk posed by an airport the FN curve $R_{FN}(n)$ is defined as [22, 24]: *"The probability that a group of n or more third party persons will be fatally injured due to the direct consequences of an aircraft accident during a given annum."*, i.e. for $n \ge 1$:

$$\begin{aligned} R_{FN}(n) &= 1 - \prod_d \left[1 - P\{n_F^d \ge n\}\right]^{N_d} \\ &\cong \sum_d \left[N_d P\{n_F^d \ge n\}\right] \end{aligned} \quad (2.2)$$

where n_F^d is the number of third party fatalities due to an accident of a type d flight. Some literature sources, e.g. [26] refer to "*more than n*", which defines $R_{FN}^{>}(n)$ as $R_{FN}^{>}(n) = R_{FN}(n+1)$, for $n \ge 0$.

Safety regulation of airports and hazardous installations in various countries apply an acceptability criterion on $R_{FN}(n)$ of the following form [25-27]:

$$R_{FN}(n) \le C / n^{\alpha} \quad (2.3)$$

where α is the steepness of the limit line and C a constant that determines the maximal acceptable level for $n = 1$. A steepness $\alpha = 1$ is called risk neutral (e.g. in UK); a steepness $\alpha = 2$ is called risk averse (e.g. in the Netherlands). In the latter case larger accidents are weighted more heavily and are thus only accepted with a relatively lower probability.

Another common societal risk indicator is Collective risk R_C, which is defined as

$$R_C = E\{n_F\} \quad (2.4)$$

where n_F is the number of persons in area Y that are killed or fatally injured due to the direct consequences of aircraft flight accidents during a given annum [23]. Collective risk R_C is known to be equal to a summation over the FN-curve, e.g. [24]:

$$R_C = \sum_{n=1}^{\infty} R_{FN}(n) = \sum_{n=0}^{\infty} R_{FN}^{>}(n) \quad (2.5)$$

Under the assumption that people on the ground are unprotected to a crash of a commercial aircraft, the relation between Collective risk and Individual risk is as follows [24]:

$$R_C = \int_Y R_I(y)\rho(y)dy \tag{2.6}$$

where $\rho(y)$ is the population density as a function of crash center location *y*, and *Y* is the area that may be affected by aircraft accidents.

B. TPR models for UAS operations

Literature on TPR models for UAS operations has focused on $R^i_{Cground} = E\{n^{UAS}_{F,i}\}$, where $n^{UAS}_{F,i}$ is the number of persons on the ground that are killed or fatally injured due to the *i*-th UA flight colliding to the ground. This has resulted in the following characterization [28-30]:

$$R^i_{Cground} = E\{n^{UAS}_{F,i}\} = \int_Y R^i_I(y)[1-P(S\mid y,i)]\rho(y)dy \tag{2.7}$$

where $R^i_I(y)$ is the fatality probability for an unprotected person at location *y* posed by the *i*-th flight, $P(S\mid y,i)$ is the shelter protection model and $\rho(y)$ is the population density in the area *Y* considered.

The characterization of $R^i_I(y)$ satisfies [28, 29, 30]:

$$R^i_I(y) = \sum_{e\in E}[P(e\mid i)\,p_s(y\mid i,e)\big|A(d_i,e)\big|\,P(F\mid y\in A(d_i,e))] \tag{2.8}$$

where $P(e\mid i)$ is ground crash probability of *i*-th aircraft due to event type *e*, $p_s(.\mid i,e)$ is the crash location model, $\big|A(d_i,e)\big|$ is the size of the crash impact area, $P(F\mid y\in A(d_i,e))$ is the unprotected fatality model of a crash of UAS type d_i due to event type *e*. The set *E* of possible event types *e* contains UAS system failure events as well as UAM related events, such as severe weather, loss of communication and mid-air collision.

The difference between eq. (2.7) for UAS and eq. (2.6) for commercial aircraft is that (2.7) includes shelter protection. The main difference between eq. (2.8) for UAS and eq. (2.1) for commercial aircraft is that eq. (2.1) accumulates over all annual flights, and eq. (2.8) not. Another difference is that eq. (2.8) differentiates regarding types of flight and crash event, while eq. (2.1) differentiates regarding type of flight only.

In spite of the similarity there are significant differences in the approaches used for UAS and commercial aircraft in the numerical evaluation of the product terms in these equations. For commercial aviation the numerical evaluation of eq. (2.1) is largely based on statistical modelling of accident data from the past [22]. Because for future UAS operations such accident data is not available, use has to be made of dedicated submodels, e.g. [31].

III. Novel TPR Indicators for UAS Operations

For UAS crash to the ground, [28] has characterized Individual risk $R^{UAS}_I(y)$ and Collective ground risk $R^{UAS}_{Cground}$. This is explained in subsections *A* and *B* respectively.

A. Individual Risk of UAS Operations

The definition of Individual risk $R^{UAS}_I(y)$ due to possible crashes to the ground by a UAS operation involving multiple flights is: *"The probability that an average unprotected person, who resides permanently at ground location y, would get killed or fatally injured due to the direct consequences of a ground crash by a UA flight during a given annum."*

Let *N* denote the number of UAS flights per annum over the area *Y*. Then the probability of a person at location *y* being missed by all *N* UAS flights per annum equals the product over the miss probabilities $[1-R^i_I(y)]$ for the $i=1,...,N$ UA flights. Hence, Individual risk $R^{UAS}_I(y)$ satisfies:

$$R^{UAS}_I(y) = 1-\prod_{i=1}^N[1-R^i_I(y)] \tag{3.1}$$

with $R^i_I(y)$ satisfying eq. (2.8). Often $R^{UAS}_I(y) \ll 0.1$, then eq. (3.1) can be approximated by $R^{UAS}_I(y) \cong \sum_{i=1}^N R^i_I(y)$.

The key difference between eqs. (3.1) and (2.7) is that eq. (2.7) accumulates risk over the area *Y*, while eq. (3.1) accumulates risk over all UAS flights per annum.

B. Collective Ground Risk of UAS Operations

For a UAS operation involving multiple flights per annum over an area *Y* the FN curve $R^{UAS}_{FN}(n)$ is defined as the *"The probability that in an area Y a group of n or more third party persons will be killed or fatally injured due to the direct consequences of ground crashes by UA flights during a given annum"*, i.e. for $n\geq 1$:

$$\begin{aligned} R^{UAS}_{FN}(n) &= 1-\prod_{i=1}^N[1-P\{n^{UAS}_{F,i}\geq n\}] \\ &\simeq \sum_{i=1}^N[P\{n^{UAS}_{F,i}\geq n\}] \end{aligned} \tag{3.2}$$

In contrast to a commercial aviation ground crash, for most UAS ground crashes $n^{UAS}_{F,i}$ will be zero or one.

Collective ground risk $R^{UAS}_{Cground}$ of a UAS operation involving multiple flights per annum over an area *Y* is defined as: *"The expected number of third party fatalities on the ground in a given area Y due to the direct consequences of ground crashes by UA flights during a given annum."* Hence for a UAS operation conducting *N* UA flights per annum:

$$R^{UAS}_{Cground} = \sum_{i=1}^N R^i_{Cground} \tag{3.3}$$

where $R^i_{Cground}$ satisfies eq. (2.7). Also for a UAS operation, collective ground risk equals summation over its FN-curve, i.e.

$$R^{UAS}_{Cground} = \sum_{n=1}^\infty R^{UAS}_{FN}(n) \tag{3.4}$$

Adopting FN requirement eq. (2.3) also for $R^{UAS}_{FN}(n)$ and substituting this into eq. (3.4) yields the following bound:

$$R^{UAS}_{Cground} \leq C\sum_{n=1}^\infty \frac{1}{n^\alpha} = C\zeta(\alpha) \tag{3.5}$$

where $\zeta(.)$ is the Riemann zeta function, with $\zeta(2)=\pi^2/6$

[32, p.807]. Because for UAS the FN-curve will decrease more steeply with increasing n than the FN-curve for commercial aviation, it is safe to set $\alpha = 2$ in (3.5), yielding:

$$R_{Cground}^{UAS} \le C\pi^2 / 6 = C_{CGR} \quad (3.6)$$

with C_{CGR} the acceptable level of collective ground risk.

IV. Characterization of λ_E Requirements

This section develops analytical characterizations of λ_E requirements for UAS-based parcel delivery service in a populated area. Subsection *A* does so for ELOS-based characterization. Subsections *B* and *C* do so for Collective Ground Risk (CGR) and Individual Risk (IR) based characterizations respectively. Subsequently, subsection *D* compares the three characterizes of λ_E requirements.

To develop these analytical characterizations, we follow Melnyk et al. [18] in assuming the following parameter invariance for the terms in eqs. (2.7-2.8):

A1: The population density $\rho(y)$ is location invariant, i.e. $\rho(y) = \rho$ for all $y \in Y$.

A2: The shelter protection $P(S \mid y,i)$ is location and flight invariant, i.e. $[1 - P(S \mid y,i)] = P_{\bar{S}}$ for all $y \in Y$.

A3. $\sum_{e \in E} P(e \mid i) = \lambda_E T_i$, with λ_E overall UAS system failure rate and T_i the duration of the *i*-th delivery and return flight.

A4. $p_s(y \mid i,e)$ is *e*-invariant, i.e. $p_s(y \mid i,e) = p_s(y \mid i)$

A5. $A(d,e)$ is (*d*,*e*)-invariant, i.e. $A(d,e) = A$

A6. $P(F \mid y \in A)$ is *y*-invariant, i.e. $P(F \mid y \in A) = P_F$

By using the simulation-based approach of [28] these assumptions are avoided to complement the analytical results.

A. ELOS-based λ_E Requirement

Due to A1 and A2, eq. (2.7) simplifies to:

$$R_{Cground}^{i} = E\{n_{F,i}^{UAS}\} = \rho P_{\bar{S}} \int_Y R_I^i(y)dy \quad (4.1)$$

Due to A3-A6, eq. (2.8) simplifies to:

$$R_I^i(y) = p_s(y \mid i) \; |A| P_F \; \lambda_E T_i \quad (4.2)$$

Substituting eq. (4.2) into eq. (4.1) yields:

$$\begin{aligned} R_{Cground}^{i} &= \rho P_{\bar{S}} \; |A| P_F \; \lambda_E \; T_i \int_Y p_s(y' \mid i)dy' \\ &= \rho P_{\bar{S}} \; |A| P_F \; \lambda_E T_i \end{aligned} \quad (4.3)$$

Under the ELOS principle the following inequality applies:

$$R_{Cground}^{i} \le T_i C_{ELOS} \quad (4.4)$$

with C_{ELOS} the acceptable number of fatalities per flight hour.

Substituting eq. (4.3) into eq. (4.4) and evaluation yields:

$$\rho P_{\bar{S}} \; |A| P_F \; \lambda_E \le C_{ELOS} \quad (4.5)$$

which implies the following λ_E requirement:

$$\lambda_E \le C_{ELOS} / \left[\rho P_{\bar{S}} \; |A| P_F \right] \quad (4.6)$$

Melnyk et al. [18] used eq. (4.6) to quantify ELOS-based λ_E requirements for various values for $|A| P_F$ and $\rho P_{\bar{S}}$ that are representative for different UAS classes and population types, and $C_{ELOS} = 0.76 \times 10^{-7}$ fatalities per flight hour.

B. CGR-based λ_E Requirement

Substitution of eq. (4.3) into eq. (3.3) yields for collective ground risk (CGR) of *N* UAS flights per annum:

$$R_{Cground}^{UAS} = \sum_{i=1}^{N} \left[\rho P_{\bar{S}} \; |A| P_F \; \lambda_E T_i \right] \quad (4.7)$$

To evaluate the summation over T_i a model has to be adopted regarding the parcel delivery in area *Y*. This model is formulated through the following additional assumptions:

A7. A drone delivery flight travels at speed v_{cruise} on the radial from center to delivery location and back to center.

A8. *Y* is the area within a circle of radius *R* from the delivery center.

A9. The delivery location of the *i*-th UAS flight is distributed according to probability density $p_{x_i}(y) = \rho(y) / \int_Y \rho(y')dy'$.

A10. Each person living in area *Y* receives on average $\bar{n}$ UAS-based parcel deliveries per year.

Assumptions A7-A10 correspond well with a last-mile delivery in an circular area around the service centre location. The latter two assumptions have also been adopted for the simulation based approach in [28]. Assumptions A7 and A8 are needed for the analytical characterization.

In Appendix B it is shown that evaluation of eq. (4.7) under assumptions A1-A10 yields:

$$R_{Cground}^{UAS} = \bar{n}\rho^2 P_{\bar{S}} \; |A| P_F \; \lambda_E \tfrac{4}{3}\pi R^3 / v_{cruise} \quad (4.8)$$

Substituting $R_{Cground}^{UAS} \le C_{CGR}$ in eq. (4.8) yields:

$$\bar{n}\rho^2 P_{\bar{S}} \; |A| P_F \; \lambda_E \tfrac{4}{3}\pi R^3 / v_{cruise} \le C_{CGR} \quad (4.9)$$

Evaluation of (4.9) yields the CGR-based λ_E requirement:

$$\lambda_E \le C_{CGR} / [\bar{n}\rho^2 P_{\bar{S}} \; |A| P_F \; \tfrac{4}{3}\pi R^3 / v_{cruise}] \quad (4.10)$$

C. IR-based λ_E Requirement

Substituting eq. (4.2) into $R_I^{UAS}(y) = \sum_{i=1}^{N} R_I^i(y)$ yields:

$$R_I^{UAS}(y) = |A| P_F \; \lambda_E \sum_{i=1}^{N} \left[p_s(y \mid i) \times T_i \right] \quad (4.11)$$

To evaluate the summation in (4.11), the following probabilistic crash location model is adopted:

A.11 In case of a UAS crash, the center of the crash area is uniformly distributed along the radial between delivery center

and delivery location, and is Gaussian distributed across the radial with standard deviation $\sigma_{\neg}$.
Under this additional assumption, Appendix C shows:

$$R_I^{UAS}(y) = \lambda_E \ |A|P_F \ \bar{n}\rho \left[R^2 - |y|^2\right] / (|y| v_{cruise}) \qquad (4.12)$$

Following Individual risk requirement for hazardous facilities and airports:

$$R_I^{UAS}(y) \le C_{IR} \text{ for all } |y| \ge R_{zone} \qquad (4.13)$$

with R_{zone} the radius of the zone around the delivery service point; within this zone land-use restrictions apply. Substituting eq. (4.12) in (4.13) yields for all $|y| \ge R_{zone}$:

$$\lambda_E \ |A|P_F \ \bar{n}\rho \left[R^2 - |y|^2\right] / (|y| v_{cruise}) \le C_{IR} \qquad (4.14)$$

The latter yields the following IR-based λ_E requirement:

$$\lambda_E \le C_{IR} R_{zone} v_{cruise} / \left[|A|P_F \ \bar{n}\rho \ (R^2 - R_{zone}^2)\right] \qquad (4.15)$$

D. Comparison of ELOS, CGR and IR based λ_E requirements

Table I compares the effects of various model parameters on λ_E requirements in eqs. (4.6), (4.10) and (4.15). Significant differences between ELOS-based, CGR-based and IR-based λ_E requirements concern most parameters; the only exceptions are $|A|$ and P_F. Significant differences for the CGR-based versus the ELOS-based λ_E^{-1} requirement are the quadratic effect of population density ρ and cubic effect of R , the linear effects of $\bar{n}$, and the inverse-linear of v_{cruise} . Significant differences for the IR-based versus the ELOS-based λ_E^{-1} requirement are the invariance to $P_{\bar{S}}$, the quadratic effect of R, the linear effect of $\bar{n}$ and the inverse-linear effect of R_{zone} and v_{cruise}.

TABLE I. EFFECT OF VARIOUS PARAMETERS ON ELOS-BASED, CGR-BASED AND IR-BASED λ_E^{-1} REQUIREMENTS

Parameter	ELOS-based	CGR-based	IR-based
$\|A\|$	Linear	Linear	Linear
P_F	Linear	Linear	Linear
ρ	Linear	Quadratic	Linear
$P_{\bar{S}}$	Linear	Linear	-
$\bar{n}$	-	Linear	Linear
R	-	Cubic	Quadratic
R_{zone}	-	-	~Inverse linear
v_{cruise}	-	Inverse linear	Inverse linear

E. Effect of Increasing $\bar{n}$

The differences in Table I imply that with increasing $\bar{n}$ there will be break-even points beyond which ELOS-based λ_E requirement is dominated by CGR-based or IR-based λ_E requirements. Next we characterize these break-even points.

If the ELOS based λ_E requirement is exactly satisfied, then inequality eq. (4.6) yields:

$$\lambda_E = C_{ELOS} / \left[\rho P_{\bar{S}} \ |A|P_F\right] \qquad (4.16)$$

Substitution of eq. (4.16) in eq. (4.15) yields:

$$C_{ELOS} / \left[\rho P_{\bar{S}} \ |A|P_F\right] \le C_{IR} / \left[|A|P_F \ \bar{n}\rho \ (R^2 - R_{zone}^2) / (R_{zone} v_{cruise})\right]$$

Evaluation of the latter inequality yields:

$$\bar{n} \le \frac{C_{IR} P_{\bar{S}} R_{zone} v_{cruise}}{C_{ELOS}(R^2 - R_{zone}^2)} \qquad (4.17)$$

If the mean number of parcel deliveries per year $\bar{n}$ is above the bound in (4.17), then the IR-based λ_E requirement dominates the ELOS-based λ_E requirement. Notice bound (4.17) is invariant of population density ρ ; hence this bound applies for all population densities.

Similarly, a bound on $\bar{n}$ can be derived from the CGR-based λ_E requirement eq. (4.10). Substitution of eq. (4.16) in eq. (4.10) yields:

$$C_{ELOS} / \left[\rho P_{\bar{S}} \ |A|P_F\right] \le C_{CGR} / [\bar{n}\rho^2 P_H \ |A|P_F \ \tfrac{4}{3}\pi R^3 / v_{cruise}]$$

Evaluation of this inequality yields:

$$\bar{n} \le \frac{C_{CGR} 3 v_{cruise}}{C_{ELOS} 4\pi\rho R^3} \qquad (4.18)$$

If the mean number $\bar{n}$ of parcel deliveries per year is above the bound in (4.18), then the CGR-based λ_E requirement dominates the ELOS-based λ_E requirement. In contrast to IR bound (4.17), CGR bound (4.18) depends on population density ρ.

V. EVALUATION OF LAST-MILE PARCEL DELIVERY

A. Urban, Metropolitan and Metropolitan-City areas

In this subsection we use eqs. (4.6), (4.10) and (4.15) to calculate ELOS-based, CGR-based and IR-based λ_E requirements for three population densities from [18], representing Urban area ($\rho_{urban} = 0.386 \times 10^4$ km^{-2}), Metropolitan area ($\rho_{metro} = 2.5 \times \rho_{urban}$), and Metropolitan City center ($\rho_{metro-city-center} = 2.8 \times \rho_{metro}$). Values of other model parameters are given in Table II. The CGR-value follows from eq. (3.6) with $C = 10^{-3}$ [25, 27].

Table III shows the calculated number of persons $|Y| \rho = \pi R^2 \rho$ within the radius R from the delivery center for Urban, Metropolitan and Metropolitan city center.

TABLE II. PARAMETER VALUES ASSUMED FOT THE QUANTIFIED EXAMPLE

Parameter	Value
$\|A\|$	1 m^2
P_F	1
$P_{\bar{S}}$	0.1
$\bar{n}$	[0.1,100]
R	3146 m
R_{zone}	100 m
v_{cruise}	$15 m/s$
C_{ELOS}	0.76×10^{-7} per flight hour
C_{CGR}	1.645×10^{-3} per annum
C_{IR}	1×10^{-6} per annum

TABLE III. NUMBER OF PERSONS WITHIN CIRCLE WITH RADIUS R; PARAMETER VALUES ASSUMED FOT THE QUANTIFIED EXAMPLE

Area type	Number of persons
Urban	1.2×10^5
Metropolitan	3.0×10^5
Metropolitan City Center	8.4×10^5

Figures 1-3 show the λ_E requirements as a function of mean annual UAS deliveries $\bar{n}$ per person for Urban, Metropolitan and Metropolitan City Center respectively. Using eqs. (4.17) and (4.18) the break-even points in Figures 1-3 are also shown in Table IV. Doole et al. [33] estimated for the Paris area (population of 12.3 million) the number of parcels to be UAS-delivered at 161 million, i.e. $\bar{n}=13.1$. This lies well above the ELOS take-over points in each of Figures 1 - 3.

TABLE IV. BREAK-EVEN POINTS IN FIGURES 1-3

$\bar{n}$	IR-based	CGR-based
Urban	$\bar{n}=0.8$	$\bar{n}=2.44$
Metropolitan	$\bar{n}=0.8$	$\bar{n}=0.98$
Metropolitan City Center	$\bar{n}=0.8$	$\bar{n}=0.35$

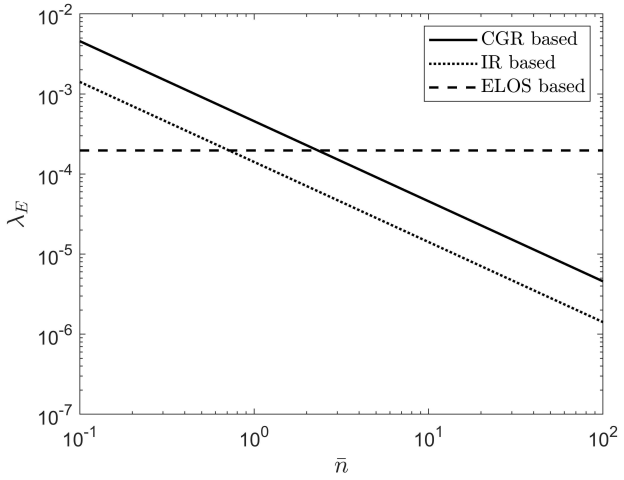

Figure 1. Urban area λ_E requirements as function of $\bar{n}$

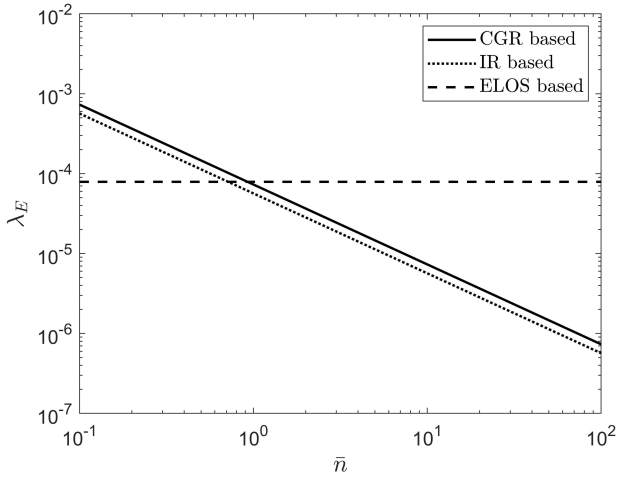

Figure 2. Metropolitan λ_E requirement as function of $\bar{n}$

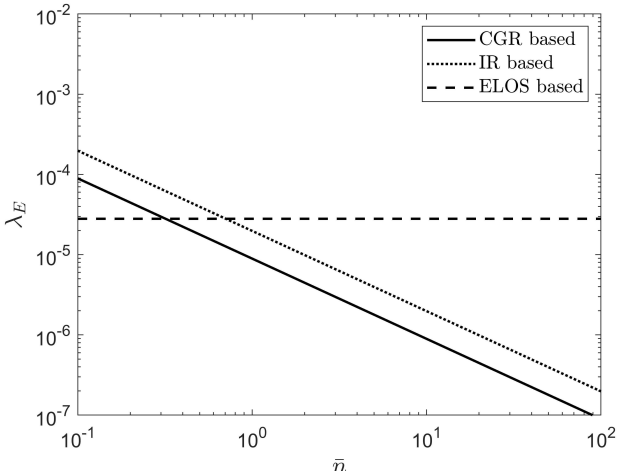

Figure 3. Metro City Center λ_E requirement as function of $\bar{n}$

B. Individual Risk contours under ELOS based requirement

Figures 4-6 present maps of Individual risk $R_I^{UAS}(y)$ under ELOS-based λ_E, for $\bar{n}=1$, $\bar{n}=10$ and $\bar{n}=100$ respectively. These maps also present contours of $R_I^{UAS}(y)=10^{-5}$, 10^{-6}. Table V shows the percentage of population within the contours in Figures 4-6.

Because the maps in Figures 4-6 compare the difference between ELOS-based and IR-based λ_E requirements, and both depend in a linear way on population density ρ (see Table I), these maps and the percentages in Table V apply to any population density, i.e. ranging from Metropolitan City Center area to Rural area.

TABLE V. POPULATION WITHIN IR CONTOURS IN FIGURES 4-6

	Figure 4 ($\bar{n}=1$)	Figure 5 ($\bar{n}=10$)	Figure 6 ($\bar{n}=100$)
$\hat{R}_I^{UAS}(y)>10^{-6}$	0.2%	19.5%	100%
$\hat{R}_I^{UAS}(y)>10^{-5}$	0.002%	0.2%	19.5%

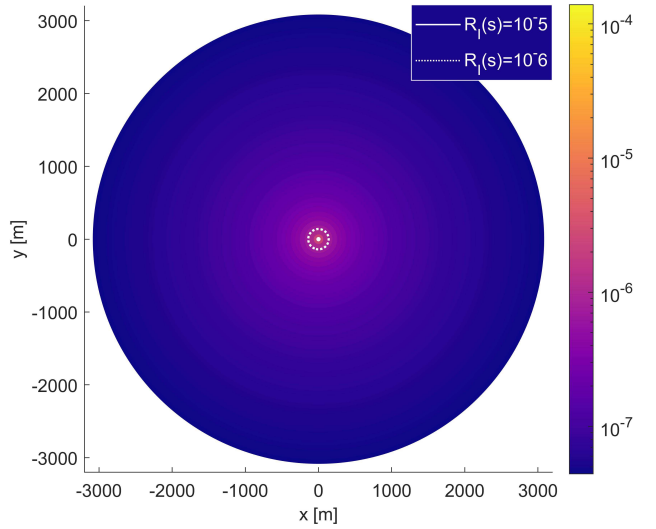

Figure 4. Map of Individual risk $R_I^{UAS}(y)$ under ELOS-based λ_E and $\bar{n}=1$. Contours are at radius of 14m and 139m from the center.

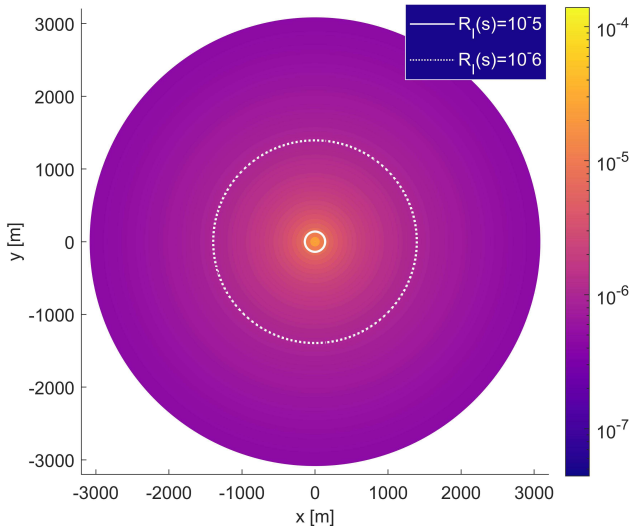

Figure 5. Map of Individual risk $R_I^{UAS}(y)$ under ELOS-based λ_E and $\bar{n}=10$. Contours are at radius of 139m and 1390m from the center.

To grasp the practical implication of the $R_I^{UAS}(y)$ maps in Figures 4 through 6, let's follow the rules for zones around Schiphol airport where the threshold value of 10^{-6} [25, 27] is not satisfied. All housing within the 10^{-5} contour have been demolished, all housing development inside the 10^{-6} contour has been banned, and a waiver has been given for the houses in between these two contours. Introducing a similar zonal policy to the maps of $R_I^{UAS}(y)$ for $\bar{n}=1$ (Figure 4) implies that 0,002% of the population in the area would have to leave their housing, and that 0.2% of the population would need a waiver to remain living in their current housing.

For $\bar{n}=10$ (Figure 5) 0.2% of the population in the area would need to leave their housing, and 19.3% of the population would need a waiver to remain living in their current housing.

For $\bar{n}=100$ (Figure 6) 19.5% would need to leave their housing, and 80.5% of the population would need to receive a waiver to remain living in their current housing. For the population the far better choice would be that the UAS to be used must satisfy the IR-based λ_E requirement.

C. *Summary of Findings*

Both ELOS-based and IR-based λ_E requirements increase linearly with increase of population density. Therefore for any population density an ELOS-based λ_E requirement poses the same IR-based bound of $\bar{n} \le 0.8$ mean number of annual UAS-based parcel deliveries per person. Figures 4-6 show that significant parts of a populated area are falling in an area with a too high individual risk level if $\bar{n}=1$, 10 and 100 respectively.

Because the CGR-based λ_E requirement increases quadratic with population density, for relative high population densities the CGR-based λ_E requirement poses a stricter bound on the allowable number of $\bar{n}$ than posed by the IR-based bound; the break-even point lies at $\rho = 1.25 \times 10^4$ km^{-2}.

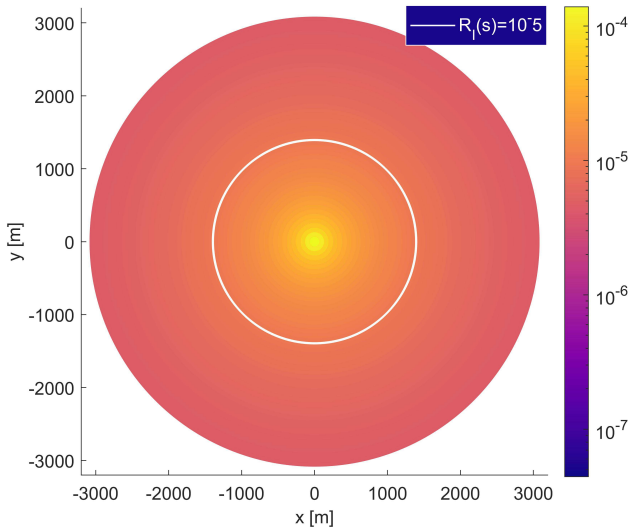

Figure 6. Map of Individual risk $R_I^{UAS}(y)$ under ELOS-based λ_E, $\bar{n}=100$. The contour of $R_I^{UAS}(y)=10^{-5}$ is at a radius of 1390m from the center.

VI. Conclusions

This paper has studied third party risk (TPR) that is posed to persons on the ground by commercial use of a UAS operation that consists of a large number of UA flights per annum, e.g. UAS based parcel delivery in an urban area. Under current regulations such commercial UAS operations over an urban area is not allowed. However with the further development of reliable small UA these operations might be proved to be sufficiently safe in future, as a result of which future regulations could allow small UA commercial operations over urban areas. From the literature review in Section II it has become clear that TPR literature has focused on the risk posed to persons on the ground per UAS flight hour. However to manage the future risk of commercial UAS operations over populated areas there is a need for TPR models that capture the risk posed to the population by a large number

of UA flights per annum. For commercial aviation the latter has been established through the use of models for Collective ground risk (CGR) and Individual risk (IR) posed to the persons on the ground. Similar model extensions in terms of Individual risk and Collective ground risk for UAS operations have been developed [28]; this is presented in Section III.

Section IV has developed an analytical characterization of λ_E requirements that are based on the novel TPR indicators for a hypothetical parcel delivery service in Urban and Metropolitan areas. Section IV also characterizes the break-even points beyond which ELOS-based λ_E requirements are dominated by CGR-based and IR-based λ_E requirements. For the IR-based λ_E requirement the break-even point does not depend on the population density.

Section V has demonstrated the use of the analytical characterizations for the evaluation of hypothetical UAS-based parcel delivery service in three types of areas: Urban area, Metropolitan area, and Metropolitan City center. For IR and CGR acceptability criterion have been based on standing regulation for hazardous facilities and airports in The Netherlands. These example evaluations show that ELOS-based λ_E requirement complies with IR-based λ_E requirement under the condition that the mean annual number of UAS-based parcel deliveries per person remains below 0.8. As is shown in section IV this 0.8 bound applies for all population densities. The break-even point of the CGR-based λ_E requirement yields an even lower bound of 0.3 for a metropolitan city center.

The analytical results in sections IV and V provide novel insights that have not been obtained using the Monte Carlo simulation framework [28]. A disadvantage of the analytical approach is the adoption of assumptions A1-A8 and A11. This means that the analytical approach strengthens the simulation based framework, though does not replace it. For example, Monte Carlo simulations remain needed to evaluate TPR when using clever UAS flying schemes, while the analytical approach is expected to be helpful in identifying the most relevant scenarios to be considered through Monte Carlo simulation.

Due to assumptions A7-A11 the developed analytical characterizations apply to the last-mile of a UAS-based parcel delivery service only. Therefore interesting follow-up research is to also develop analytical characterizations of CGR-based and IR-based λ_E requirements for third party risk of other commercial UAS-based operations, such as flying taxis and medical aid services.

Because λ_E includes the rate of mid-air collisions of a UAS with another UAS [19] and with low flying GA [20], a complementary follow-on development is the modelling and assessment of these mid-air rates and their contribution to λ_E under future UAM designs. This asks for collision risk evaluation of conflict and collision avoidance designs in future UAM operations under various uncertainties, using agent-based modelling and rare event simulation approaches that have been developed for manned air traffic [34-36].

ACKNOWLEDGMENT

The authors like to thank an anonymous reviewer for providing useful suggestions in improving the paper. This research did not receive any specific grant from funding agencies in the public, commercial or not-for-profit sectors.

APPENDIX A. LIST OF SYMBOLS

$A(.)$ or A	Crash impact area
$\lvert A(.)\rvert$ or $\lvert A\rvert$	Size of crash impact area
C	Threshold posed on FN-curve at n=1
C_{CGR}	Threshold posed on Collective Ground Risk
C_{ELOS}	Threshold posed by Equivalent Level of Safety
C_{IR}	Threshold posed on Individual Risk
d_i	UA type of *i*-th flight
e	Type of event causing UA crash to the ground
E	Set of possible UA crash causing event types
$E\{.\}$	Expectation of {.}
i	UA flight numbering
$\bar{n}$	Average annual number of UAS-based parcel deliveries per person
N_d	Annual number of commercial flights of type d
n_F^d	Number of third party fatalities due to an accident of a commercial flight of type d
$n_{F,i}^{UAS}$	Number of third party fatalities on the ground due to a ground crash of i-th UA flight
$p_s(.\mid d)$	Probability density function of the crash location s of a commercial flight of type d
$p_s(.\mid i,e)$	Probability density function of the crash location s of the *i*-th UA flight under event type e
$p_s(.\mid i)$	e-invariant version of $p_s(.\mid i,e)$
$p_{x_i}(.\mid i)$	Probability density function of the delivery location x_i of the *i*-th UAS flight
$P(e\mid i)$	Probability that the *i*-th UA flight crashes to the ground due to event type e
$P(C\mid d)$	Accident probability of commercial flight of type d
$P(F\mid y\in A(d))$	Probability that a ground crash of a commercial flight of type d is fatal for an unprotected average person at location *y* in the crash impact area
$P(F\mid y\in A(d_i,e))$	Probability that a ground crash of the *i*–th UA flight due to event type *e* is fatal for an unprotected average person at location *y* in the crash impact area
$P(S\mid y,i)$	Probability that a person at location y is sheltered against a crash of the *i*-th UA flight
P_F	(y,d_i,e) -invariant version of $P(F\mid y\in A(d_i,e))$
$P_{\bar{S}}$	(y,i) -invariant version of $1-P(S\mid y,i)$
R	Radius of hypothetical parcel delivery area
R_C	Collective risk of annual commercial flights
$R_{Cground}^i$	Collective ground risk posed by *i*-th UA flight
$R_{Cground}^{UAS}$	Collective ground risk posed by annual UA flights
$R_{FN}(n)$	FN-curve posed by annual commercial flights
$R_{FN}^{UAS}(n)$	FN-curve posed by annual UAS flights
$R_I(y)$	Individual risk posed by annual commercial flights to an unprotected average person at ground location *y*
$R_I^i(y)$	Individual risk posed by the *i*-th UAS flight to an unprotected average person at ground location *y*

$R_I^{UAS}(y)$	Individual risk posed by annual UAS flights to an unprotected average person at ground location *y*
R_{zone}	Radius of zone where land-use restrictions apply
s	Location of centre of UA crash area
T_i	Duration of *i*-th UAS delivery flight (incl. return flight)
v_{cruise}	Cruise speed of UA delivery flight
y	Ground location of an unprotected average human
Y	Population area considered
Y_{Zone}	Zone for which land-use restrictions apply
α	Threshold posed on steepness of FN-curve
$\rho(y)$	Population density as a function of ground location *y*
$\zeta(.)$	Riemann zeta function
λ_E	Overall UAS system failure rate

APPENDIX B. DERIVATION OF EQ. (4.8)

For very large *N*, eq. (4.7) equals:

$$R_{Cground}^{UAS} = \sum_{i=1}^{N}\left[\rho P_{\bar{S}}\ |A|P_F\ \lambda_E T_i\right] = \rho P_{\bar{S}}\ |A|P_F\ \lambda_E N\bar{T} \qquad (B.1)$$

with

$$\bar{T} = E\{T_i\} = \int_Y T_i\, p_{x_i}(x_i)dx_i \qquad (B.2)$$

where $p_{x_i}(.)$ is the probability density function of the delivery location x_i of the *i*-th delivery flight in delivery area Y.

Due to A7: $T_i = 2|x_i|/v_{cruise}$; hence eq. (B.2) becomes:

$$\bar{T} = \int_Y 2|x_i|/v_{cruise}\ p_{x_i}(x_i)\ dx_i \qquad (B.3)$$

In view of A8 we express x_i in the polar system $x_i = (r_i\cos\theta_i,\ r_i\sin\theta_i)$; hence

$$p_{r_i,\theta_i}(r_i,\theta_i) = |J|\, p_{x_i}(r_i\cos\theta_i,\ r_i\sin\theta_i) \qquad (B.4)$$

with

$$|J| = (r_i\cos\theta_i\cos\theta_i + r_i\sin\theta_i\sin\theta_i) = r_i \qquad (B.5)$$

This yields a transformation of eq. (B.3) to:

$$\bar{T} = \int_0^R\int_0^{2\pi} 2r_i^2/v_{cruise}\ p_{x_i}(r_i\cos\theta_i,\ r_i\sin\theta_i)\ dr_i d\theta_i \qquad (B.6)$$

Due to A1 and A9: $p_{x_i}(r_i\cos\theta_i,\ r_i\sin\theta_i) = 1/(\pi R^2)$; hence

$$\bar{T} = \int_0^R\int_0^{2\pi} 2r_i^2/(\pi R^2 v_{cruise})\ dr_i d\theta_i = \int_0^R 4r_i^2/(R^2 v_{cruise})dr_i$$

$$= \frac{4}{R^2 v_{cruise}}\tfrac{1}{3}r_i^3\Big|_0^R = \tfrac{4}{3}R/v_{cruise} \qquad (B.7)$$

Substituting eq. (B.7) in eq. (B.1) yields:

$$R_{Cground}^{UAS} = \rho P_{\bar{S}}\ |A|P_F\ \lambda_E N\tfrac{4}{3}R/v_{cruise} \qquad (B.8)$$

Due to A10 the annual number *N* of UAS-based parcel delivery return flights in area Y equals:

$$N = \bar{n}\rho\ |Y| \qquad (B.9)$$

Substituting (B.9) in (B.8) and evaluation yields for all $y \in Y$:

$$R_{Cground}^{UAS} = \bar{n}\ |Y|\rho^2 P_{\bar{S}}\ |A|P_F\ \lambda_E \tfrac{4}{3}R/v_{cruise}$$

Substituting $|Y| = \pi R^2$ and subsequent evaluation yields (4.8).

APPENDIX C. DERIVATION OF EQ. (4.12)

For large *N*, the summation in eq. (4.11) can be replaced by an $N\times E\{T_i p_s(y|x_i)\}$, i.e.

$$R_I^{UAS}(y) = |A|P_F\ \lambda_E \sum_{i=1}^{N}\left[p_s(y|i)\times T_i\right]$$

$$= |A|P_F\lambda_E\ N\ E\{T_i p_s(y|x_i)\}$$

$$= \lambda_E\ |A|P_F\ N\int_Y T_i p_s(y|x_i)p_{x_i}(x_i)dx_i \qquad (C.1)$$

Due to A8 and A9, the integration over *Y* transforms to:

$$R_I^{UAS}(y) = \lambda_E\ |A|P_F\ N\int_0^R\int_0^{2\pi} T_i p_s(y|r_i,\theta_i)\frac{r_i}{\pi R^2}dr_i d\theta_i \qquad (C.2)$$

Due to A11 we express both *s* and *y* in the polar system $s = (s_r\cos s_\theta,\ s_r\sin s_\theta)$ and $y = (y_r\cos y_\theta,\ y_r\sin y_\theta)$. Hence

$$p_{s_r,s_\theta}(y_r,y_\theta|r_i,\theta_i) = |J|\, p_s(y_r\cos y_\theta, y_r\sin y_\theta|r_i,\theta_i) \qquad (C.3)$$

with

$$|J| = (y_r\cos y_\theta\cos y_\theta + y_r\sin y_\theta\sin y_\theta) = y_r \qquad (C.4)$$

Substituting eq. (C.4) in eq. (C.3) and subsequent evaluation yields for $y_r > 0$:

$$p_s(y_r\cos y_\theta,\ s_r\sin y_\theta|r_i,\theta_i) = p_{s_r,s_\theta}(y_r,y_\theta|r_i,\theta_i)/y_r \qquad (C.5)$$

Next we decompose $p_{s_r,s_\theta}(y_r,y_\theta|r_i,\theta_i)$ as follows:

$$p_{s_r,s_\theta}(y_r,y_\theta|r_i,\theta_i) = p_{s_\theta}(y_\theta|y_r,r_i,\theta_i)\,p_{s_r}(y_r|r_i,\theta_i) \qquad (C.6)$$

Due to A11, we have:

$$p_{s_r}(y_r|r_i,\theta_i) = 1(y_r \le r_i)/r_i$$

$$p_{s_\theta}(y_\theta|y_r,r_i,\theta_i) = N\{y_\theta;\theta_i,\sigma_\neg/y_r\}$$

Substituting the latter two equations in eq. (C.6) yields:

$$p_{s_r,s_\theta}(y_r,y_\theta|r_i,\theta_i) = N\{y_\theta;\theta_i,\sigma_\neg/y_r\}1(y_r \le r_i)/r_i \qquad (C.7)$$

Substituting eq. (C.7) in eq. (C.5) yields for $y_r > 0$:

$$p_s(y_r\cos y_\theta,\ s_r\sin y_\theta|r_i,\theta_i) = N\{y_\theta;\theta_i,\sigma_\neg/y_r\}1(y_r \le r_i)/(r_i y_r)$$

Substituting this into (B.2) and subsequent evaluation yields:

$$R_I^{UAS}(y) = \lambda_E\ |A|P_F\ N\int_0^R\int_0^{2\pi} T_i\ N\{y_\theta;\theta_i,\sigma_\neg/y_r\}\ \frac{1(|y|\le r_i)}{|y|\pi R^2}\ dr_i d\theta_i$$

$$= \lambda_E \ |A|P_F \ N \int_0^R T_i \ \frac{1(|y| \le r_i)}{|y|\pi R^2} \ dr_i$$

$$= \lambda_E \ |A|P_F \ N \frac{1}{|y|\pi R^2} \int_{|y|}^R T_i dr_i \qquad \text{(C.8)}$$

Substituting $T_i = 2r_i / v_{cruise}$ into eq. (B.8) yields:

$$R_I^{UAS}(y) = \lambda_E \ |A|P_F \ N \frac{1}{|y|\pi R^2} \int_{|y|}^R (2r_i / v_{cruise}) dr_i$$

$$= \lambda_E \ |A|P_F \ N \frac{1}{|y|\pi R^2} \left[r_i^2 / v_{cruise}\Big|_{r_i=R} - r_i^2 / v_{cruise}\Big|_{r_i=|y|} \right]$$

$$= \lambda_E \ |A|P_F \ N \frac{1}{|y|\pi R^2} \left[R^2 - |y|^2 \right] / v_{cruise} \qquad \text{(C.9)}$$

Substituting eq. (B.9) in eq. (C.9) yields:

$$R_I^{UAS}(y) = \lambda_E \ |A|P_F \ \bar{n}\rho \ |Y| \frac{1}{|y|\pi R^2} \left[R^2 - |y|^2 \right] / v_{cruise} \qquad \text{(C.10)}$$

Substituting $|Y| = \pi R^2$ in eq. (C.10) yields eq. (4.12).

REFERENCES

[1] ICAO, 2011, Unmanned Aircraft Systems (UAS), Circular 328-AN/190, International Civil Aviation Organization.

[2] EASA, 2021, Study on the societal acceptance of Urban Air Mobility in Europe, 19th May 19, 2021

[3] FAA, "Operation and Certification of Small Unmanned Aircraft Systems," Department of Transportation, Washington, USA, 2016.

[4] JARUS, Guidelines on Specific Operation Risk Assessment (SORA), Joint Authorities Regulation Unmanned Systems, 2017.

[5] S. Oh, J. Cho, N. Kim, Y. Yoon, Preliminary impact assessment of restricting airspace over populated areas for sUAS operation, 99th Transportation Research Board Conf., January 2020.

[6] E. Petritoli, F. Leccese, L. Ciani, Reliability and maintenance analysis of unmanned aerial vehicles, Sensors, Vol. 18 (2018), pp. 3171-3186.

[7] S. Primatesta, A. Rizzo, A. La Cour-Harbo, Ground risk map for Unmanned Aircraft in urban environments, J. of Intelligent & Robotic Systems, May 2019, pp. 489-509.

[8] C.A. Ippolito, Dynamic ground risk mitigating flight conyrol for autonomous small UAS in urban environments, AIAA-Aviation Forum, 17-21 June 2019, Dallas, Texas.

[9] E. Ancel, F.M. Capristan, J.V. Foster, R.C. Condotta, In-time non-participant casualty risk assessment to support onboard decision making for autonomous unmanned aircraft, AIAA-Aviation Forum, June 2019.

[10] X. Hu, B. Pang, F. Dai, K.H. Low, Risk assessment model for UAV cost-effective path planning in urban environments, IEEE Access, Vol. 8 (2020), pp. 150162-150173.

[11] EC, 2021, Commision implementing regulation on a regulatory framework for the U-Space, 22nd April 2021.

[12] R.A. Clothier, B.P. Williams, K.J. Hayhurst, Modelling the risks remotely piloted aircraft pose to people on the ground, Safety Science, Vol. 101 (2018), pp. 33-47.

[13] C. Jiang, H.A.P. Blom, A. Sharphanskykh, Third Party Risk Indicators and Their Use in Safety Regulations for UAS Operations, AIAA Aviation Forum, June 2020.

[14] R.E. Weibel and R.J. Hansman Jr., "Safety Considerations for Operation of Different Classes of UAVs in the NAS," Unmanned Unlimited, Technical Conf., Workshop and Exhibit, 20-23 Sept. 2004, Chicago, IL, AIAA-2004-6421, pp. 1-11.

[15] C. Lum and B. Waggoner, "A Risk Based Paradigm and Model for Unmanned Aerial Systems in the National Airspace," AIAA Conf., Seatle, 2010.

[16] K. Dalamagkidis, K. Valavanis and L. Piegl, "On integrating unmanned aircraft systems into the National Airspace System, Springer, 2012.

[17] R. Clothier and R. Walker, "Determination and Evaluation of UAV Safety Objectives," Proc. 21st Int. UAV Systems Conf., 2006, pp. 18.1-18.16.

[18] R. Melnyk, D. Schrage, V. Volovoi and H. Jimenez, "A third-party casualty risk model for unmanned aircraft system operations," Reliability Engineering & System Safety, Vol. 124 (2014), pp. 105-116.

[19] S.H. Kim, Third-Party Risk Analysis of Small Unmanned Aircraft Systems Operations, J. of Aerospace Information Systems, Vol. 17 (2020), pp. 24-35.

[20] A. La Cour-Harbo, H. Schioler, Probability of low-altitude midair collision between general aviation and unmanned aircraft, Risk Analysis, Vol. 39 (2019), pp. 2499-2513.

[21] H. Bohnenblust, Risk-based decision making in the transportation sector, In: R.E. Jorissen, P.J.M. Stallen (Eds.), Quantified Societal Risk and Policy Making, Kluwer Academic Publishers, Dordrecht, 1998.

[22] B.J.M. Ale and M. Piers, The assessment and management of third party risk around a major airport, Journal of Hazardous Materials, Volume 71, Issues 1–3, January 2000, pp. 1-16.

[23] H. Smets, Frequency distribution of the consequences of accidents involving hazardous substances in OECD countries, 1996, Etudes et Dossiers, Geneva Association.

[24] G.M.H. Laheij, J.G. Post, B.J.M. Ale, Standard methods for land-use planning to determine the effects on societal risk, J. of Hazardous Materials, Vol. 71 (2000), pp. 269–282.

[25] P.H. Bottelberghs, Risk analysis and safety policy developments in The Netherlands, J. of Hazardous Materials, Vol. 71 (2000), pp. 59–84.

[26] S.N. Jonkman, P.H.A.J.M. Van Gelder, J.K. Vrijling, An overview of quantitative risk measures for loss of life and economic damage, J. of Hazardous materials, Vol. A99 (2003), pp. 1-30.

[27] V.M. Trbojevic, Risk criteria in EU, Proc. ESREL 2005, Poland, 27-30 June 2005.

[28] H.A.P. Blom, C. Jiang, W. Grimme, M. Miticia, Y. Cheung, Third Party Risk modelling of Unmanned Aircrafy System operations, with application to parcel delivery service, Reliability Engineering and System Safety, accepted June 2021.

[29] S. Bertrand, N. Raballand, F. Viguier, F. Muller, Ground risk assessment for long-range inspection missions of railways by UA's, Proc. 2017 Int. Conf. on Unmanned Aircraft Systems, Miami, FL.

[30] E. Ancel, F. Capristan, J. Foster and R. Condotta, Real-time risk assessment framework for unmanned aircraft system (UAS) traffic management (UTM), 17th AIAA ATIO Conf., 2017, AIAA-2017-3273.

[31] A. La Cour-Harbo, Quantifying risk of ground impact fatalities for small unmanned aircraft, J. of Intelligent and Robotic Systems, Vol. 93 (2019), pp. 367-384.

[32] M. Abramowitz and I.A. Stegun (eds.), Handbook of Mathematical Functions, National Bureau of Standards, 10th printing, December 1972.

[33] M. Doole, J. Ellerbroek and J. Hoekstra, "Drone Delivery - Urban airspace traffic density estimation," TU Delft, Delft, 2018.

[34] H.A.P. Blom, G. J. Bakker, Safety Evaluation of Advanced Self-Separation Under Very High En Route Traffic Demand, Journal of Aerospace Information Systems, Vol. 12, No. 6 (2015), pp. 413-427. doi: 10.2514/1.I010243

[35] M. Mitici and H.A.P. Blom, Mathematical models for air traffic conflict and collision probability estimation, IEEE Transactions on Intelligent Transportation, Vol. 20 (2019), pp. 1052-1068.

[36] S.H. Stroeve, H.A.P. Blom, C. Hernandez Medel, C. Garcia Daroca, A. Arroyo Cebeira. S. Drozdowski, Modelling and simulation of intrinsic uncertainties in validation of collision avoidance systems, J. of Air Transportation, Vol. 28 (2020), pp. 173-183, DOI: 10.2514/1.D0187